

# Clinical and automatic evaluation of the severity of maculopathy using optical coherence tomography

H.I. Abdelkader<sup>1</sup>, Mona Abdelkader<sup>2</sup>, Fahmi Khalifa<sup>3</sup>, Doaa.gabr<sup>4</sup>

**Abstract-** Diabetic Macular Edema is characterized according to Early Treatment Diabetic Retinopathy studies by thickening of macula. The search included two mains. Firstly, a study included comparing the retinal thickness measurements using two scanning Optical Coherence Tomography (OCT) mechanisms (Radial scan – Three dimension (3D) scan) of patient with Diabetic macular edema (DME) and normal subjects, correlates between retinal thickness measurements with 3D and radial in different types of DME. Finally, an algorithm has been proposed for the detection of DME from OCT image in order to be early diagnosed and have proper treatment. Fourteen healthy individual with 27 eyes and 23 patients with 46 eyes. All subjects were examined using two scanning methods of Spectral domain OCT. The retinal thickness (RT) from two scans was measured, recorded and compared for every level of maculopathy. The mean and standard deviation (SD) were evaluated using statistical package for social science (SPSS.16). The correlation between two scans are calculated using Pearson's correlation coefficient. The result of these study showed that DME can be detected using OCT. RT thickness of DME is different from those of normal eyes. The comparison between radial and 3D-OCT scan reported that there was no-significant difference between the mean retinal thicknesses of the two scans through the nine macular region ( $p > 0.5$ ). The quality image showed a significant difference between two scans ( $p = 0.024$ ,  $p = 0.040$ ) in case of cystoid and mixed edema respectively. Significant correlation was found through the nine macular region between two scans in case of cystoid, mixed, diffuse edema and normal subjects. Artificial Neural Network classification of DME yielded highest accuracy 96.43%, sensitivity 100% and specificity 92.86%. Thus, ophthalmologists can use this algorithm by in early detection of macular edema.

**Keywords:** Diabetic Macular edema, Optical Coherence Tomography, Artificial Neural Network, Retinal thickness measurements.

**Abbreviations:** Optical Coherence Tomography; RT: Retinal Thickness; DME: Diabetic Macular Edema; OCT: ANN: Artificial Neural Network; GLCM: Gray Level Co-occurrence Matrix

1- Associate Prof. Physics department, faculty of science  
Mansoura University. Email: hikader5@yahoo.com

2- Associate Prof. Mansoura Ophthalmic Center, faculty of medicine  
Mansoura University. Email: monaabdeldkader78@yahoo.com

3- Associate Prof. Communication department, faculty of Engineering  
Mansoura University. Email: Fahmikhalifa@yahoo.com

4- MSC Research Student. Faculty of science  
Mansoura University. Email: doaa.gabr.sci@gmail.com

## 1 Introduction:-

Retina is a thin clear and accurate light sensible tissue which locates at the back of the human eye. Macula, is a small portion of the retina responsible for detailed central vision. Several diseases may affect the retina .Severity of diseases may vary from blurred vision to vision loss. Diabetic retinopathy (DR) is one of such diseases .One of the most severe complications of diabetes is DR. DR may lead to seep of blood vessels and accumulation of fluids in the macular region leading to formation of DME.

DME is the most common cause of the ocular acuteness loss in diabetes. [1] DME usually develops at any time during progression of (DR). DR is associated with high blood glucose levels that cause damage to the vessels supplying blood to the retina.[2-3] DME is characterized by thickening of the macula, hard exudate (HE) and blot hemorrhage (HA )according to ETRDs. [4]

Clinically, the severity of DME is divided into two main classes, clinically significant macular edema (CSME) and non-clinically significant macular (Non-CSME). Non-CSME is a moderate class of DME, and CSME is the acute class of DME. [2-3]The ocular acuteness may be improve if DME was early detected and treated. Different imaging techniques have been used for the diagnosis of DME such as Color Fundus photographs, Fluorescein Angiography (FA), Retinal Thickness Analyzer (RTA) and Optical Coherence Tomography (OCT).

Optical coherence tomography depicted firstly by Huang et al. in 1991 [5] as an imaging instrument able to render depth-resolved structural images of the retina. Optical coherence tomography is able to detect DME at an earlier stage. [6].OCT has the ability to proceed cross sectional imaging with high resolution and analysis of structural changes in the eye during disease development. OCT permits an important estimation of Diabetic macular edema with efficiency in both qualitative and quantitative characterization of DME. So OCT be a standard tool in the diagnosis of patients with DME. [7].OCT gives an accurate and useful data that will be used for better diagnose and follow DME.

The aim of this work is to compare the retinal thickness measurements of 3D- OCT scan and retinal thickness measurements for radial OCT scan for patients with DME and normal subjects and correlate between retinal thickness measurements with 3D- OCT scan and radial-OCT scan in different types of DME. Secondly, a method has been introduced for the detection of DME from OCT image in order to be early diagnosed and have proper treatment.

## 2 Subjects and methods:-

### Part (I):-

The study was carried out in Mansoura Ophthalmic center after obtaining approval of Mansoura Ethic community. Informed consents were also obtained from all participating subjects after the explanation of the study was given to participating. Inclusion criteria for study were diabetes mellitus, clinical evidence of diabetic maculopathy. OCT scans were captured using spectral domain OCT [Topcon 3D-OCT 1000 Mark II, Tokyo, Japan, software version 3.20].

The study was divided into two groups: The first group included 14 healthy individual (5 males and 9 females) aged between 40-60 years with 27 eyes. The second group included 23 patients (10 males and 13 females) aged between 45-65 years with 46eyes as shown in table (1). Fluorescein angiography (Topcon corporation, 2000, TRC, 5011, japan) was done to evaluate the level of maculopathy (Focal, Diffuse, Mixed and cystoid macular edema).So, all eyes must undergo at least one fluorescein angiographic evaluation of the level of maculopathy. Exclusion criteria included eyes with other pathologies (hemorrhage, retinal detachment, retinal venous occlusion, age related macular degeneration, choroid neovascularization, and high myopia).

### Optical coherence tomography:-

Optical coherence tomography is a powerful noninvasive imaging instrument works similar to ultrasound imaging. The spectral domain optical coherence tomography (SD-OCT) measuring principle is based on spectral interferometry. A low coherence source light is directed into a 2x2 fiber optic coupler. The coupler splits the incident optical power evenly into sample and reference arm. Exiting light from the reference fiber is incident upon a reference delay element and redirected back into the same fiber. Exiting light from the sample fiber is incident upon a scanning mechanism prepared to focus the beam on the sample and to scan the focused spot in one or two lateral directions. The sample and reference beam are combined by fiber optic coupler. On the surface of a photo-receiver or detector, the combined light is made to interfere. The signal is analyzed by the OCT spectrometer. The spectrometer consists of a collimator, transparent or reflective grating, focusing lens and the CCD camera. An attenuating filter is added in order to prevent reaching the saturation level of charge couple device (CCD) camera. The line scan CCD camera will acquire the A-scan data. A-scan is map of reflectivity of the sample along an axial depth direction. Computer convert the signal by the (Fast Fourier Transform) to develop a depth B scan image (combination of a series A-scan). [8-11]

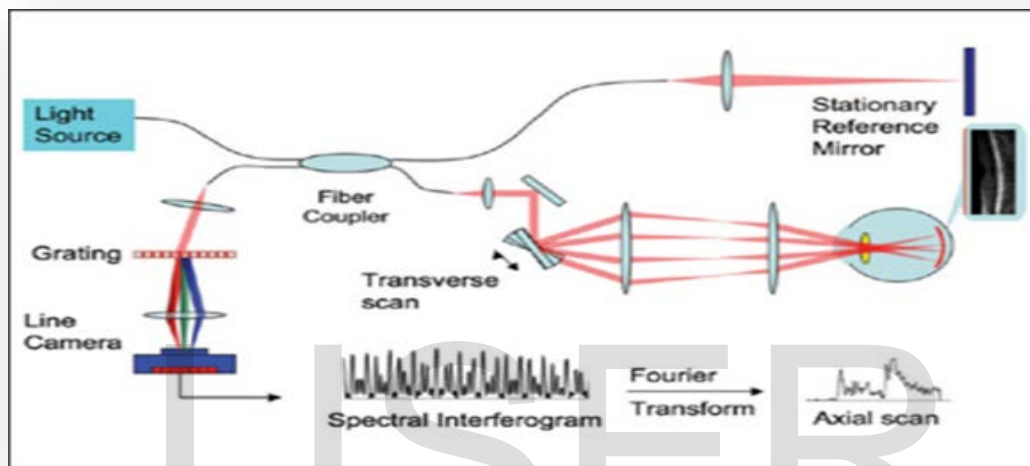


**Figure (1) spectral domain OCT.**

### Measurements protocols:-

The pupil were dilated with tropicamide eye drop 1% before the OCT measurements. The technician selects the proper fixation method for subjects. The technician select the suitable fixation protocols button (Disc, Disc and macula, and Macula). There are three scanning protocols 3D scans, radial scans, and raster scans. All subjects were suspected to be scanned with spectral domain OCT using macula protocols. Each measurement sitting started with placing a subject head upright on the chin of the instrument. The data were collected using OCT shown in figure (4). It works on the principle of spectral low coherence interferometry using 840nm super-luminescent diode laser. We use both the 3D scan as shown in figure (3-a) and fast macular thickness radial scan as shown in figure(3-b). For radial scan 12 B scan of 6mm length were obtained centered at the fovea at 30° separate angles. Each B-scan consisted of 1024 longitudinal A-scan and for 3D-scan, 128 B-scan of 6x6 mm length were obtained. Each B-scan consists of 512 longitudinal A-scan. Machines analysis software automatically identify the retinal boundaries. All scans were evaluated for boundary misalignment by the scan operator. No misalignment of these boundaries was observed. All scans of both 2 methods were included for analysis. Both 12 scans of radial scan and 128 scan of 3D-scan were recalculated by machines software. Subsequently, it is generates a topographic macula map divided into 9 areas as defined by Early Treatment Diabetic Retinopathy studies divided into one central area, four para-foveal areas and four peri-foveal areas as shown in figure(2)

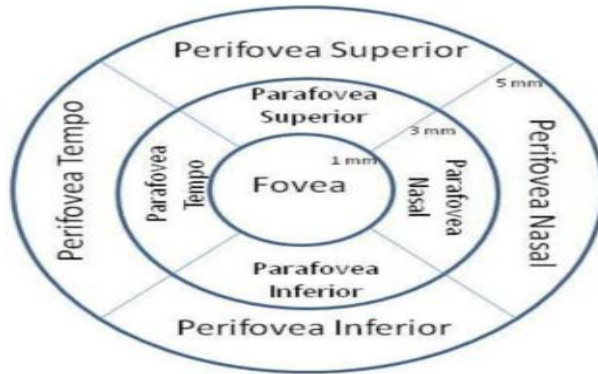


Figure (2) Different Regions of ETDRS (central fovea, parafovea ,perifovea) and diameter of each regions.

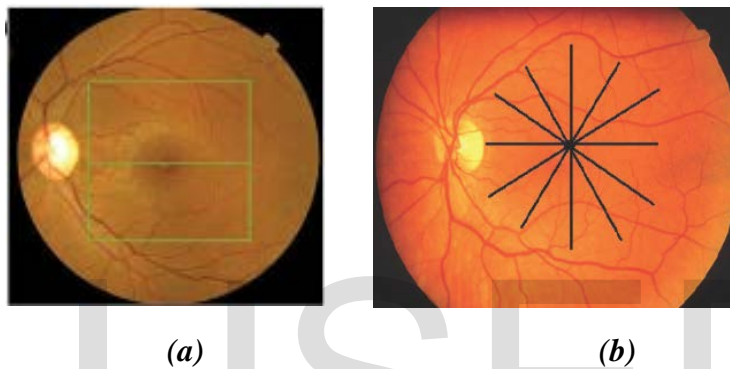


Figure (3) (a)-the macula with 3D scan centered at the fovea, (b)-the macula with 6 radial scan centered at the fovea



Figure (4) Topcon1000

SDOCT

## Part (II):-

### A-DME detection method:-

### Region of interest extraction (ROI) and Image enhancement:-

Firstly, the input images (3D OCT scan) are cropped to evolve the OCT region of interest and discarding the not required region. Input OCT images is in RGB format (three color components namely red, green and blue) shown in figure (5-a), figure (6-a). The RGB images are converted to gray scale images. Then, these filtered and smoothed using median filter shown in figure (5-b), figure (6-b).

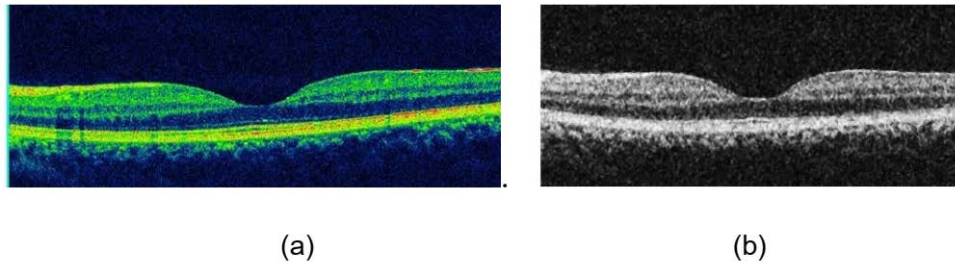


Figure (5) (a)-normal OCT, (b) normal OCT image after pre-processing

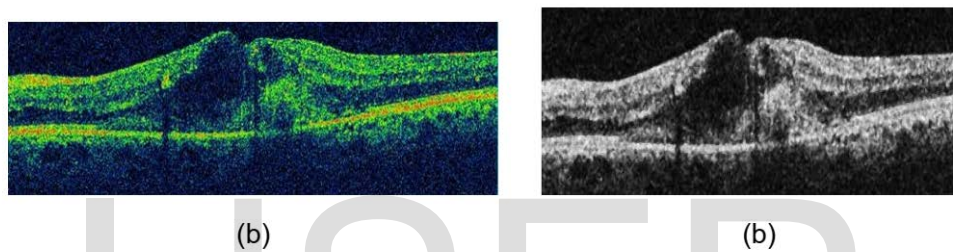


Figure (6) (a) disease OCT, (b) disease OCT image after preprocessing

### 2-segmentation using graph based theory: -

The retina consist of ten layers. Only two layers is our interest to be segmented. These layers are Inner Limiting Membrane (ILM) and Retinal Pigment Epithelium (RPE). Segmentation is the process of sectioning a digital image into a set of pixels or regions. Each OCT image is a digital image consists of a set of pixel and segmented those pixels on the basis of the similar characteristic like, color, intensity and texture. Segmentation target is to transform the representation of an image into something more important and simple to analyze. Segmentation of image can be achieved by finding edges or points or line in the image. Graph based algorithm have several good features in workable applications. Each OCT image is represents in terms of a graph of nodes where every pixel in the image belongs to a node in the graph. And the graph based segmentation is based on choosing edges from the graph of nodes. [12] Edges are the links connected the nodes. Weights on each edge measure the dissimilarity between pixels and specified to individual edges to form track priority as in equation (1).

$$W_{ab} = 2 - (g_a + g_b) + W_{min} \quad \rightarrow 1$$

Where,

$W_{ab}$  is the weight referred to the edge linking nodes a and b.



$g_a$  is the vertical gradient of the image at node a,  
 $g_b$  is the vertical gradient of the image at node b,  
 $w_{min}$  is the minimum weight in the graph which is a small positive number added for system stabilization

Equation (1) give low weight values to node pairs with large vertical gradients. In our implementation,  $g_a$  and  $g_b$  are normalized to values between 0 and 1, and  $w_{min} = 1 \times 10^{-5}$ .

To go across the graph from a starting node to a terminus node, the chosen track is the path with a minimum total weight sum . The resulting track is the cut which detaches one region from another. [13] The key to precisely detaching a graph is to specify the suitable edge weights. Popular metrics for varying weight values involve functions of distances between pixels or differences between intensity values [14]. To trace this required path, Dijkstra's shortest path search algorithm [15] is used to divide the image graph into layers. The necessary layers are then plotted. The result of segmentation and plots of ILM and RPE layers is shown in Figure (7).

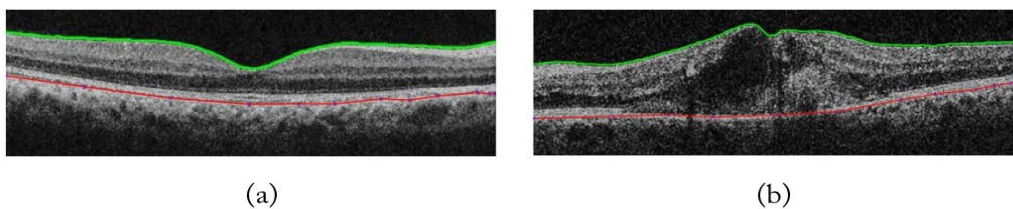


Figure (7) (a) Normal image, and (b) disease image with marketed RBE and ILM

### 3-Thickness evaluation:-

Diabetic macular edema manifestation causes change in the thickness of retinal layers. The average thickness of the region between (ILM) and (RBE) are evaluated for detection of DME. The resulting thickness didn't show much variation between normal and diseased image. So, this weakness is avoided by sectioning the segmented images into five equal regions as shown in figure (8),(9). The average thickness for each region between (ILM) and (RPE) is evaluated. The central region of retinal image represent the fovea region. The thickness measure of the fovea region is relatively higher for the image with DME and low for normal image.

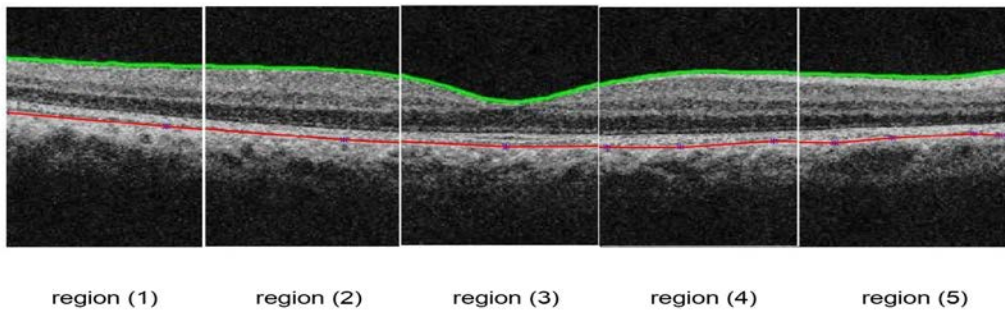


Figure (8) normal segmented image split into five regions.

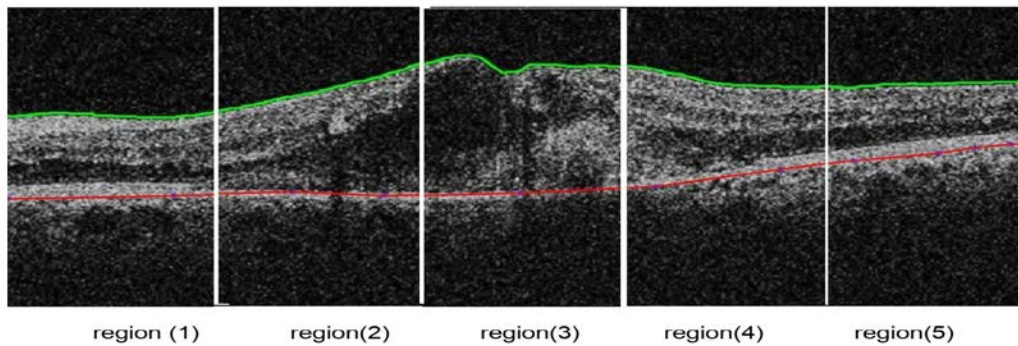


Figure (9) diseased segmented image split into five regions.

### Texture features:-

Texture analysis is an important component useful for characterizing objects or regions in an image. Texture analysis is a significant tool in medical imaging studies which is a method for image analysis and classification. Texture analysis is capable of analysis image for many medical imaging application. The texture analysis information is given in a set of "gray tone spatial dependency matrices" called Gray Level Co-occurrence matrix (GLCM). From these matrix a number of textural features of the image can be computed. These features is called Haralick features. [16-17] In this work a few of these features are extracted from OCT image such as Contrast, Energy, Entropy, Homogeneity, correlation, Dissimilarities, Sum of variance, Sum square of variance, Sum of average and difference entropy. These features besides the thickness evaluation are used for training of the artificial neural network classifier to distinguish between normal and diseased OCT image.

### Energy:-

Energy is obtained from the square root of Angular Second Moment texture feature (ASM). It gives the sum of square element in GLCM, also known as uniformity. Its range [0 1]. Energy reaches its highest value, when gray level distribution has either or periodic form

$$Energy = \sum_{i=0}^{M-1} \sum_{j=0}^{N-1} P(i,j)^2$$

Where

$p$  : The matrix element of the input is image,  $(i, j)$  is pixels of the matrix and

$(M, N)$ : the dimension of the image.

### Entropy:-

Entropy is fully distinct from energy. It measures the disturbance of an image .It attained its largest value when all elements in the matrix (p) are equal. Entropy is inversely proportional to GLCM energy.

$$Entropy = - \sum_{i=0}^{M-1} \sum_{j=0}^{N-1} P(i, j) \log p(i, j)$$

### Contrast:-

Contrast is a measure gray level change between two pixels present in an image. Local intensity variation in an image that will support contributions from  $p(i, j)$  away from the diagonal i.e.  $i \neq j$ .

$$Contrast = \sum_{i=0}^{M-1} \sum_{j=0}^{N-1} [i - j]^2 p(i, j)$$

### Homogeneity:-

Image homogeneity measure from inverse difference moment. And it indicate the value that measure the closeness of distribution of elements in the GLCM and passes this value to the diagonal GLCM. Opposite of homogeneity weight value is contrast weight value.

$$Homogenit = \sum_{i=0}^{M-1} \sum_{j=0}^{N-1} \frac{p(i, j)}{1 + (i - j)^2}$$

### Correlation:-

It is a measure of the dependence of gray level in co-occurrence matrix.

$$Correlation = \sum_{i=0}^{M-1} \sum_{j=0}^{N-1} \frac{(ij) p(i, j) - \mu_x \mu_y}{\sigma_x \sigma_y}$$

Where  $\mu_x \mu_y$  and,  $\sigma_x \sigma_y$  are the means and standard deviations.

### Sum square of variance:-

Sum square of variance is another name of contrast which measure the variation in intensity, and it puts comparatively high weights on the elements that vary from the average value of  $P(i, j)$ .

$$Variance = \sum_{i=0}^{M-1} \sum_{j=0}^{N-1} (i - \mu)^2 p(i, j)$$

### Sum of variance:-

$$\text{sum of variance} = \sum_{i=2}^{2Ng} (i - f)^2 P_{x+y}(i)$$

Where  $f \sum_{i=2}^{2Ng} i p_{x+y}(i)$



**Sum of average:-**

$$\text{Sum of average} = \sum_{i=2}^{2Ng} x + y(i)$$

**Difference entropy:-**

$$\text{difference entropy} = - \sum_{i=0}^{Ng-1} p_{x-y}(i) \log\{p_{x-y} - (i)\}$$

**Dissimilarities:-**

$$\text{Dissimilarities} = \sum_{i=0}^{M-1} \sum_{j=0}^{N-1} [i - j] p(i, j)$$

**Artificial neural network (ANN):-**

Neural network (NN) means the linkage between neurons exist in different layers of the system. NN consist of three layer. The input layer which correspond to the number of inputs neurons of neural network (biological synapse), hidden layer (more synapse) and output layer which correspond to the number of the output values of the NN (biological axon). [18]

Artificial neural network (ANN) can be defined based on some character such as, number of neurons, weights setting between the neurons, training the network and evaluating the results and activation function used in various layer shown in figure (10).

For our ANN, It is made of  $x_1, x_2, \dots, \dots, x_m$ . Neurons in the input layer ( $i$ ). Each neuron in the input layer has a weight  $w_1, w_2, \dots, w_m$  connected to a neuron in the hidden layer ( $j$ ). Hidden layer accept data from the input layer. The linkage between each hidden layer and input layer is characterized by a weight value  $W_{ij}$ . The input neuron is modified by multiplying the incoming signal with weight value gives  $w_1x_1, w_2x_2, \dots, w_mx_m$  and summing these weights  $\sum_{i=1}^m w_i x_i$

$$v = w_1x_1 + w_2x_2 + \dots + w_mx_m = \sum_{i=1}^m w_i x_i$$

Where  $v$  is the weighted sum

The weights are adjusted to obtain the required output. To get the required output with reduced error, output ranges between 0 and 1, algorithms are used to adjust the weight of artificial neural network and this process is called training. [19]

The output of neuron ( $y$ ) is a function of the weighted sum and the equation below is called the activation function

$$y = f(v)$$

Where  $f(v)$  is equal to

$$f(v) = a + v = a + \sum_{i=1}^m w_i x_i$$

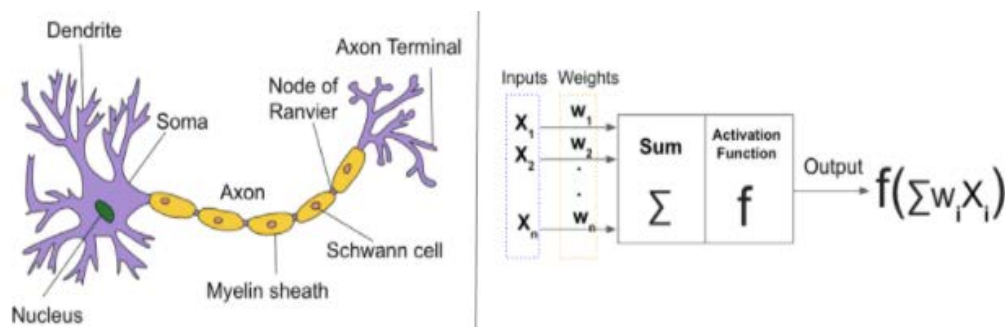


Figure (10) Artificial Neural Network schematic diagram.

ANN is trained with samples (OCT images) labelled with the class they belong to where normal image labelled with 0 and diseased image labelled with 1. The ANN is trained with eleven features .we are able to classify diseased image and image without disease.

**3 Results:-**

**Part (1):-**

The study included 37 subjects: fourteen were normal and twenty three were diagnosed with maculopathy. Age and sex were included in table (1). All normal subjects were free of any symptoms except one eye is neglected because of high-myopia. Retinal thickness map for radial scan OCT and 3D scan OCT were recorded and analyzed for each eye of every subjects.

**Statistical analysis**

Data were analyzed using statistical package for social science (spss.16) for windows evaluation version. T-test analysis was used to determine the statistical significance of the thickness change between 3D-OCT and radial OCT scan in eyes with maculopathy.  $P < 0.05$  was taken to represent a significant difference. The correlation coefficient between two scans is underwent using Pearson's correlation coefficient.

Types of groups	Sex		Number of eyes	Number of subject	Age
	male	Female			
First control group	5	9	27 eyes	14	40-60
Second study group	10	13	46 eyes	23	
Cystoid			16	8	
Diffuse			10	5	
Focal			10	5	
Mixed			10	5	

Table (1) the clinical Data of Subject

### 3D OCT Scan and Radial OCT scan :-

The comparison of retinal thickness map included 9 region of the macula of both radial OCT scan and 3D –OCT scan were summarized (Mean ± SD) in tables (2-6) below. For normal eyes in table (2) figure (11), there was no-significant difference between the mean retinal thicknesses of the two scans through the nine macular region. The quality of the two mechanisms was significantly different (P=0.002).

Macula region	Radial scan	3D scan	P-value
Centre	180.38±19.08	181.88±19.76	<b>0.811</b>
Inner temporal	194.25±9.90	190.75±11.16	<b>0.888</b>
Inner nasal	209.75±7.11	206.5±7.73	<b>0.742</b>
Inner superior	208.50±9	206.38±7.76	<b>0.687</b>
Inner inferior	205.62±7.69	203.5±9.21	<b>0.515</b>
Outer temporal	153.38±3.96	149.75±3.06	<b>0.590</b>
Outer nasal	183.25±5.92	181.50±9.91	<b>0.190</b>
Outer superior	167.50±7.54	164.5±8.38	<b>0.422</b>
Outer inferior	161.25±7.52	156.25±6.84	<b>0.909</b>
Average thickness	203.83±3.92	200.58±5.73	<b>0.153</b>
Quality	60±26	47.5±10.39	<b>0.002</b>

Table (2) Thickness of normal macula in (µm) in both radial and 3D-scan OCT.

For eyes with focal edema in table (3) figure (12), there was no-significant difference between the retinal thicknesses of the two scans through the nine macula region. There was no significant difference between the qualities of two mechanism.

Macula region	Radial scan	3D scan	P-value
Centre	256±62.75	245.33±57.54	<b>0.711</b>
Inner temporal	288±11.79	297.67±14.50	<b>0.852</b>
Inner nasal	336.33±28.94	326.33±37.17	<b>0.544</b>
Inner superior	306±26	308.67±7.77	<b>0.057</b>
Inner inferior	303.33±39.11	314.67±31.36	<b>0.813</b>
Outer temporal	254.33±13.05	255±5.26	<b>0.141</b>
Outer nasal	349±64.02	354.67±83.07	<b>0.562</b>
Outer superior	261.67±5.51	287.33±29.14	<b>0.063</b>
Outer inferior	276.33±11.50	267.33±17.62	<b>0.501</b>
Average thickness	289.73±16.74	294.60±24	<b>0.710</b>
Quality	41.67±25.89	39±12.49	<b>0.184</b>

Table (3) thickness of focal macular edema in (µm) in both radial and 3-Dscans

For eyes with diffuse edema in table (4) figure (13), there was no-significant difference between the retinal thicknesses of the two scans through the nine macula region .There was no significant between the qualities of two mechanism.

Macula region	Radial	3D-scan	P-value
<b>Centre</b>	231.83 ±40.09	226.17±32.60	<b>0.490</b>
<b>Inner temporal</b>	285.17 ±30.97	284.58±31.27	<b>0.920</b>
<b>Inner nasal</b>	296.67 ±28.71	295.17±29.29	<b>0.971</b>
<b>Inner superior</b>	299 ±30.55	298±29.33	<b>0.671</b>
<b>Inner inferior</b>	293 ±31.04	292.58±33.99	<b>0.829</b>
<b>Outer temporal</b>	241.33 ±27.32	238.5±23.64	<b>0.739</b>
<b>Outer nasal</b>	268.33 ±24.79	266.92±23.31	<b>0.766</b>
<b>Outer superior</b>	235 ±69.02	250.08±17.11	<b>0.239</b>
<b>Outer inferior</b>	249.83 ±23.97	248.92±24.92	<b>0.830</b>
<b>Average thickness</b>	261.24±24.09	259.69±23.21	<b>0.827</b>
<b>Quality</b>	78.50±11.11	43.75±6.68	<b>0.055</b>

Table (4) thickness of diffuse macular edema in (µm) in both radial and 3-Dscans.

For eyes with mixed edema in table (5) figure (14), there was no-significant difference between the mean retinal thicknesses of the two scans through the nine macula region. The quality of the two mechanisms was significantly different (P=0.040)

Macula region	Radial	3D-scan	P-value
<b>Centre</b>	278.27±45.19	262.18±59.93	0.355
<b>Inner temporal</b>	311.09±55.45	314±35.69	0.062
<b>Inner nasal</b>	301.55±50.37	308.73±44.38	0.893
<b>Inner superior</b>	298±33.26	300.91±14.38	0.124
<b>Inner inferior</b>	312.36±40.69	308.64±46.70	0.729
<b>Outer temporal</b>	272.73±53.34	277.18±48.25	0.825
<b>Outer nasal</b>	280.9±33.15	281.91±22.44	0.536
<b>Outer superior</b>	253.9±28.71	254.73±20.27	0.317
<b>Outer inferior</b>	269.6±30.67	250.91±83.40	0.364
<b>Average thickness</b>	277.65±29.16	278.81±83.46	0.848
<b>Quality</b>	40.82±25.69	35.55±10.03	0.040

Table (5): thickness of mixed macular edema in (µm) in both radial and 3-Dscans

For eyes with cystoid edema in table (6) figure (15), there was no-significant difference between the mean retinal thickness of the two scans through the nine macula region .The quality of the two mechanisms was significantly different (P=0.024).

Macula region	Radial	3D-scan	P-value
Centre	419.47±187.5	423.07±188.74	0.932
Inner temporal	384.67±130.68	400.13±128.97	0.939
Inner nasal	396.47±109.5	398.13±103.7	0.833
Inner superior	384.67±119.45	407.27±129.23	0.773
Inner inferior	385.8±105.33	385.53±100.88	0.758
Outer temporal	300.8±65.35	322.73±87.07	0.859
Outer nasal	325.13±55.03	336.8±54.43	0.900
Outer superior	314.5±68.6	320.67±71.57	0.727
Outer inferior	302.47±45.82	300.07±52.04	0.478
average thickness	331.21±66.40	341.30±67.56	0.914
Quality	34.93±16.12	34±6.66	0.024

Table (6): thickness of cystoid macular edema in (µm) in both radial and 3-Dscans.

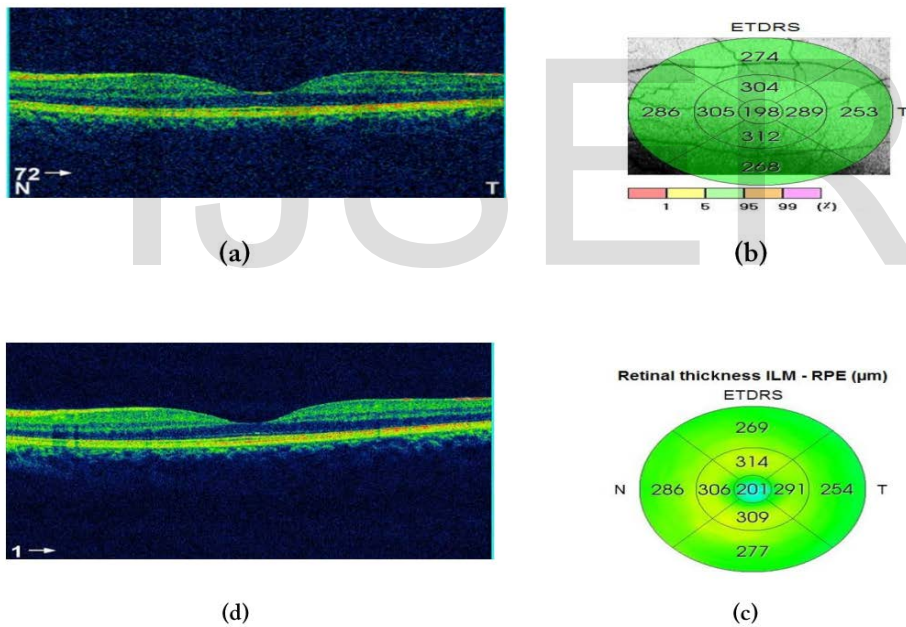
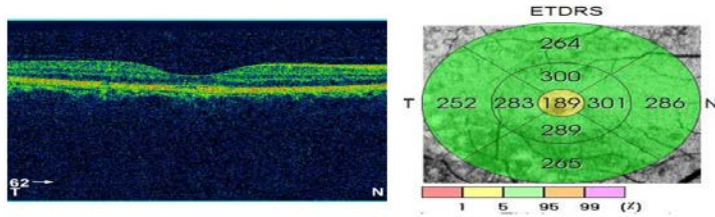


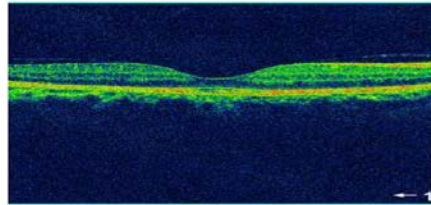
Figure (11) a,b OCT shows normal macula and thickness map of 3D -scans respectively .c, d OCT shows normal macula and thickness map of radial scans respectively.



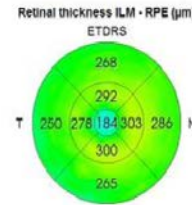


(a)

(b)

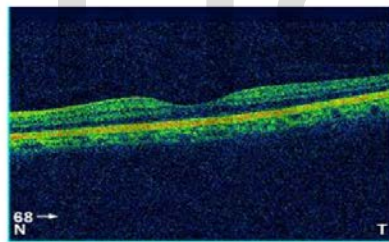


(c)

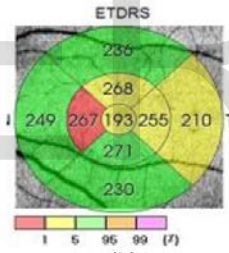


(d)

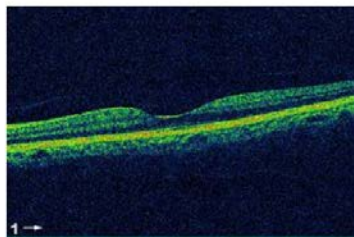
Figure (12) a, b OCT shows focal macula and thickness map of 3D- scans respectively .c, d OCT shows focal macula and thickness map of radial scans



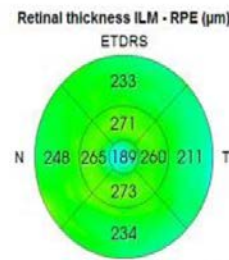
(a)



(b)



(c)



(d)

Figure (13) a, b OCT shows diffuse macula and thickness map of 3D- scans respectively .c, d OCT shows diffuse macula and thickness map of radial scans.

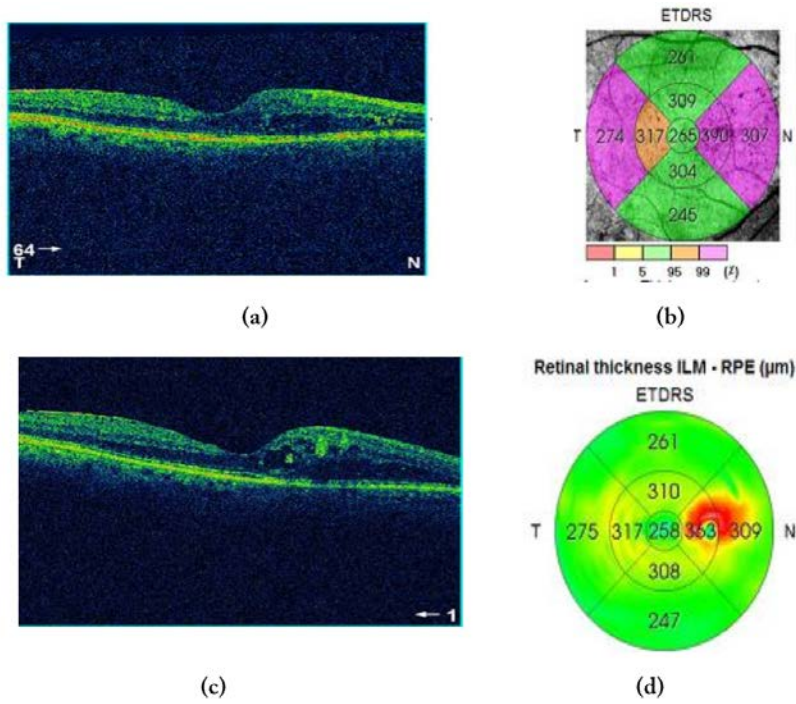


Figure (14) a,b OCT shows mixed macula and thickness map of 3D- scans respectively .c, d OCT shows mixed macula and thickness map of radial scans.

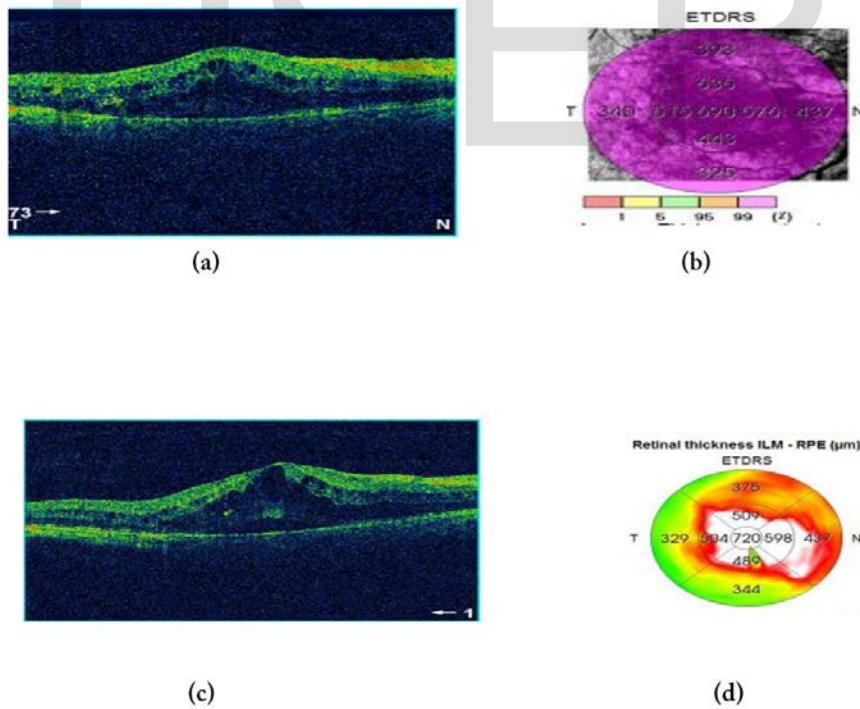


Figure (15) a, b OCT shows cystoid macula and thickness map of 3D- scans respectively .c, d OCT shows cystoid macula and thickness map of radial scans.

### Correlation between 3-D scans and radial scans

The formula used to calculate Pearson's correlation coefficient( $r$ ) is shown below

$$r = \frac{1}{n-1} \frac{(xi-\bar{x})(yi-\bar{y})}{SxSy}$$

The value  $r$  ranges between +1 and -1, if  $r > 0$  indicates a positive relation between X and Y: as one gets larger, the other gets larger, if  $r < 0$  indicates a negative relationship: as one gets larger, the other gets smaller and if  $r = 0$  indicate no relationship.

Correlation of cystoid radial and 3-D scan	correlation value	p value
<b>Centre</b>	0.924	0.000
<b>Inner temporal</b>	0.505	0.055
<b>Inner nasal</b>	0.932	0.000
<b>Inner superior</b>	0.815	0.000
<b>Inner inferior</b>	0.794	0.000
<b>Outer temporal</b>	0.085	0.764
<b>Outer nasal</b>	0.860	0.000
<b>Outer superior</b>	0.508	0.053
<b>Outer inferior</b>	0.663	0.007
<b>Average thickness</b>	0.635	0.011
<b>Quality image</b>	0.437	0.103

Table (7) Correlation Coefficient (Pearson's( $r$ )) for thickness of 3-D and radial OCT scans in case of cystoid macular edema.

In table (7), in eyes with cystoid edema, the central and inner nasal macular thickness of both mechanism 3D-OCT and radial OCT is highly correlated ( $r = 0.924$ ,  $r = 0.923$ ) respectively. The inner temporal macular thickness is with moderate correlation ( $r = 0.505$ ). The inner superior and inner inferior is with strong correlation ( $r = 0.813$ ,  $r = 0.794$ ) respectively. The quality image is with low correlation ( $r = 0.437$ )

Correlation of mixed radial and 3- D scan	Correlation value	p-value
<b>Centre</b>	0.572	0.066
<b>Inner temporal</b>	0.826	0.002
<b>Inner nasal</b>	0.707	0.015
<b>Inner superior</b>	0.426	0.192
<b>Inner inferior</b>	0.771	0.006
<b>Outer temporal</b>	0.609	0.047
<b>Outer nasal</b>	0.646	0.032
<b>Outer superior</b>	0.571	0.066
<b>Outer inferior</b>	0.532	0.092
<b>Average thickness</b>	0.584	0.059
<b>Quality image</b>	0.546	0.082

Table (8) Correlation Coefficient (Pearson's( $r$ )) for thickness of 3-D and radial scans in case of mixed macular edema

In table (8) in eyes with mixed edema, the central macular thickness is with moderate correlation in both mechanisms 3D-OCT and radial OCT ( $r = 0.572$ ). The inner temporal and inner inferior macular thickness is with strong correlation ( $r = 0.826$ ,  $r =$

0.771) respectively. The inner nasal thickness is with moderate correlation ( $r = 0.707$ ).The inner superior is with low correlation ( $r = 0.426$ ). The quality of image is with moderate correlation ( $r=0.546$ )

Correlation of diffuse radial and 3-d scan	Correlation value	p-value
Centre	0.850	0.000
Inner temporal	0.992	0.000
Inner nasal	0.971	0.000
Inner superior	0.970	0.000
Inner inferior	0.974	0.000
Outer temporal	0.965	0.000
Outer nasal	0.957	0.000
Outer superior	0.651	0.022
Outer inferior	0.934	0.000
Average thickness	0.989	0.000
Quality image	0.694	0.012

Table (9) Correlation Coefficient (Pearson's(r) for thickness of 3-D and radial scans in case of diffuse macular edema.

In table (9) in eyes with diffuse edema, the central, inner temporal, inner nasal, inner superior and inner inferior is with strong correlation in both 3D- OCT and radial OCT scan. ( $r = 0.850, r = 0.992, r = 0.971, r = 970, r = 0.974$ ) respectively. The quality image is with moderate correlation ( $r=0.694$ ).

Correlation of focal radial and 3d scan	Correlation value	p-value
Centre	- 0.077	0.885
Inner temporal	- 0.232	0.659
Inner nasal	0.274	0.599
Inner superior	- 0.503	0.309
Inner inferior	0.516	0.294
Outer temporal	-0.075	0.887
Outer nasal	0.272	0.602
Outer superior	- 0.657	0.157
Outer inferior	- 0.343	0.505
Average thickness	0.165	0.755
Quality image	- 0.676	0.141

Table (10) Correlation Coefficient (Pearson's(r) for thickness of 3-D and radial scans in case of focal macular edema.

In table (10), in eyes with focal edema, the central and inner temporal macular thickness is with no linear association in both 3D- OCT and radial OCT. ( $r = - 0.077, r = - 0.232$ ) respectively. The inner nasal is with weak correlation ( $r = 0.274$ ).The inner superior

is with moderate negative correlation ( $r = - 0.503$ ). The inner inferior is with moderate correlation( $r = 0.516$ ). The quality of image is with moderate negative correlation ( $r = - 0.676$ ).

Correlation of normal radial and 3-d scan	Correlation value	p-value
Centre	0.950	0.000
Inner temporal	0.855	0.007
Inner nasal	0.903	0.002
Inner superior	0.701	0.053
Inner inferior	0.909	0.002
Outer temporal	0.197	0.639
Outer nasal	0.951	0.000
Outer superior	0.838-	0.009
Outer inferior	0.643	0.085
Average thickness	0.707	0.050
Quality image	0.733	0.038

Table (11) Correlation Coefficient (Pearson's(r) for thickness of 3-D and radial scans in case of normal volunteers.

In table (11), for normal eyes, the central, inner temporal, inner nasal, inner inferior macular thickness is with strong correlation in 3D-OCT and radial OCT( $r = 0.950$ ,  $r = 0.855$ ,  $r = 0.903$ ,  $r = 0.909$ ) and the inner superior is with moderate correlation( $r = 0.701$ ). The quality image is with moderate correlation( $r = 0.733$ ).

## Part II:-

Seventy three OCT collected images which is divided in two group. The first group included 23 patient diagnosed with DME (bilateral) and the second group included 14 normal (bilateral). The ANN is trained using 45 images in which 13 normal and 32 DME. During testing 28 images are used consists of 14 normal and 14 diseased. Output of the classifier is evaluated based on the value of

**True Negative (TN):-** Number of normal image predicted as normal.

**True positive (TP):-**Number of abnormal predicted as abnormal.

**False positive (FP):-** Number of normal predicted as abnormal.

**False negative (FN):-** Number of abnormal predicted as normal.

Using these value, the performance of our classifier is evaluated using medical calculation program (NCSS .12)



<b>Number of neuron=15</b>	<b>Object predicted Absent(Normal)</b>	<b>Object predicted Present(Diseased)</b>
<b>Object Actually Absent(Normal)</b>	True Negative (T <sub>N</sub> ) (13)	False Positive(F <sub>P</sub> ) (1)
<b>Object Actually Present(Diseased)</b>	False Negative(F <sub>N</sub> ) (0)	True positive (T <sub>P</sub> ) (14)

Table (17) output of the classifier

**Sensitivity and specificity:-**

**Sensitivity (Sn) or True positive Rate:-**

Measure of existence of abnormality in the image out of the total number of images with abnormalities.

$$Sensitivity = \frac{T_p}{T_p + F_N} \times 100$$

Where

T<sub>p</sub>: true positive

F<sub>N</sub>: false negative

**Specificity (Sp) or True Negative rate:-**

Measure of the existence of abnormality in the image out of the total number of images without abnormality.

$$specificity = \frac{T_N}{F_P + T_N} \times 100$$

Where

T<sub>N</sub>: true negative value

F<sub>P</sub>: False positive value

**Accuracy (A):-**

Measure of existence or obscurity of the abnormalities in the image out of the total number of images.

$$Accuracy = \frac{T_p + T_N}{(T_p + F_N + F_P + T_N)} \times 100$$

The number of test images, classification results and the corresponding sensitivity, specificity and accuracy are shown in table (18). ANN classification of DME gives highest accuracy 96.43%, sensitivity 100% and specificity 92.86%

<b>Number of test image</b>	<b>28</b>
<b>Number of normal images</b>	<b>14</b>
<b>Number of abnormal images</b>	<b>14</b>
<b>Sensitivity</b>	<b>100%</b>
<b>Specificity</b>	<b>92.86%</b>
<b>Accuracy</b>	<b>96.43%</b>
<b>True positive</b>	<b>14</b>
<b>True negative</b>	<b>13</b>
<b>False positive</b>	<b>1</b>
<b>False negative</b>	<b>0</b>

Table (18) classification results

## Discussion

Optical coherence tomography is a diagnostic tool which used for examination of retina and objective measurements of retinal thickness [20-21]. OCT reinforced the capability to diagnose and guide treatment decision in retinal diseases. OCT gives us new insights about the retinal morphological change and quantitative estimating of retinal thickness in case of diabetic retinopathy [22]. Retinal thickness (RT) is automatically calculated by computer software and are presented in color coded topographic retinal thickness maps. RT is defined as the distance between the ILM and RBE and is calculated for nine regions include one central macular region, inner and outer region each divided into four quadrant known as Early Treatment Diabetic Retinopathy Studies (ETDRs). ETDRs defined DME as focal, diffuse, cystoid retinal thickening in the macular area. In this study, the retinal thickness measurements is based on the radial OCT and 3D-OCT scan using Topcon 1000 OCT. There was no significant difference between the two scans through the nine macular region in eyes characterized with DME and normal subjects. There is only a significant difference between the quality of two scans in eyes with mixed and cystoid ( $p = 0.040$ ,  $p = 0.024$ ) respectively.

Kaori Sayanagi [23] observed that there was no significant difference in the RT between 3D and 6 radial line scans except the center subfield using the Topcon OCT-1000, and inner inferior and outer nasal areas on the Canon SPOCT in the eyes with macular diseases and found also that there was no significant difference between the different scans on both SD-OCT devices in the healthy subjects,.

Farzin Forooghian [24] reported that macular thickness in nine retinal subfields and macular volume were significantly higher in the Cirrus HD-OCT system compared with the Stratus OCT system .

In this study, in case of eyes with cystoid macular edema, there was statically significant correlation between the thickness measurements of the radial and 3D-OCT central macular region ( $r = 0.924$   $p = 0.000$ ). In case of eyes with mixed, there was statically no-significant correlation between the thickness measurements of the radial and 3D-OCT in central macular region ( $r = 0.572$ ,  $p = 0.066$ ). In case of eyes with diffuse, there was statically significant correlation between the thickness measurements of the radial and 3D-OCT central macular region ( $r = 0.850$ ,  $p = 0.000$ ). In case of eyes with focal there was statically no-significant correlation between the thickness measurements of the radial and 3D-OCT central macular region ( $r = - 0.077$ ,  $p = 0.885$ ). In case of normal eyes, there was statically significant correlation between the thickness measurements of the radial and 3D-OCT central macular region ( $r = - 0.950$ ,  $p = 0.000$ ).

Antonio Polito [25] found that the interclass coefficient of retinal thickness measurements with fast macular thickness mapping of the stratus OCT were always greater than 0.80 and 0.98 in healthy subjects and diabetic patients with CSME respectively.

3D -OCT scan and radial scan generate the early treatment diabetic retinopathy study grid with thickness values displayed in each sector. Browning [26] said that Central macular region has important diagnostic value.

The automated segmentation boundary is the same between radial and 3D- scan. As it define the distance from ILM to RPE. So, we need to consider other factors to explain the difference between the two scans. The first factor is different number of sampling point between radial and 3D-scan. The radial scan calculate the RT by analyzing (1024 A-scan  $\times$ 12 B-scan) while 3D-scan calculate thickness by analyzing (512 A-scan  $\times$ 128 B-scan). The number of the retinal points analyzed in the radial scan is lower than those with 3D-scan, however, the sampling density of the radial scan in the central macular region is greater than that of 3D-scan. As a consequence the radial scan may miss a region of interest if it is not with one of the 12 Linear B scan. Whereas 3D scan should not. The acquisition time of the radial scan (0.3or 0.5 second) is shorter than that of 3D-scan (3.5 or 2.7 seconds). Because of long acquisition time, the 3D – OCT scan may subject to movements or image artifacts causing error in the measurements or segmentation algorithm failure especially in eyes with severe macular edema.[23]

OCT is a valuable tool in medicine that provide non-invasive mapping anatomy of the retina. This technology have greatly increased knowledge of normal and diseased anatomy for medical research and is an important in diagnose and treatment planning. OCT retinal images needed the use of computers to facilitate processing and analysis. Computer algorithms particularly uses for the delineation of anatomical structures and other region of interest. Image segmentation algorithms plays a vital role in diagnose, localization of the pathology, study of anatomical structures and treating planning. [27]

In the current study, we introduce a new method for automated detection of DME from retinal images for proper diagnosis and treatment. Appropriate segmentation of retinal is very important for extraction the retinal layers of interest. This has been done by using graph based method for segmentation of ILM and RBE of the retina. Thickness is evaluated and features has been extracted for the segmented image after it has been splitted into five sections. Then, it has been classified. As classification is a machine learning that require to section a feature space derived from the image by using data with known labels. Classifiers are known as supervised methods because they require training data .that are manually segmented and then used as references for automatically segmenting new data [28-29]. So that, to facilitate these problem of classification, Artificial Neural Network will be introduced.

Artificial neural network (ANN) are used in many areas such as neuroscience, mathematics, physics, electrical and computer engineering. ANN is copying of the human brain. For human brain, it is a part of the central nervous system (CNV). It is a highly complex organ that control the entire body .It is capable of storing and managing information received by the sense organs. The brain are made of many cells called neurons .A neuron is like a switch with the input and output information. The neuron is consist of cell body, axon and dendrites. The dendrites of neurons receive information (electro-chemical) signals to and from the cell by a special connection called synapses. [30]

The ANN is a parallel network of processing elements that stimulate biological learning which attained through the adaption of weights referred to the connection between nodes. The ultimate use of ANN is as a classifier in medical imaging in which the weights are determined by using training data and the ANN is then used to segment new data.[27]

Namita Sengar et al. [31] have graded Macular Edema by dividing the fundus image into regions based on international standard. They have located macula using adaptive method. Severity of the disease is found based on scaling of bright lesions in the macular region. This method has achieved an accuracy of 80 to 90 %. Aditya Kunwar et al. [32] have detected high risk macular edema region by considering a region of radius 1DD around the macula. This region is found to cover exudates present in high risk region with good accuracy. They have tried to reduce the computational time without compromising accuracy of detection.

Pratul P.Srinivasan et al. [33], have proposed SD – OCT based method that uses feature vectors extracted from multi-scale histograms of oriented gradient descriptors and have classified it using support vector machine. The algorithm has been found to be useful for remote diagnosis of ophthalmic diseases. Umer Aftab et al. [34] have developed an automated system for detection of exudates color fundus images. They have created a binary map for the candidate exudates region using Gabor filter band. The images have been classified using Gaussian mixture model.

M. Usman Akram et al. [35] have proposed a system for accurate detection of macula using a detailed feature set and GMM based classifier. They have also developed a hybrid classifier which is a combination of GMM and SVM. This method has improved accuracy in exudate detection.

Qi Yang et al [36] used a dual scale gradient information based segmentation of macular region in OCT image. This method give good accuracy and reproducibility.

Bilal Hassan et al [37] assessed Macular Edema by a fully automated method using discriminating analysis classifier. Sheela. N et al [38] has been proposed method of automated detection of DME from retinal image using Support Vector Machine. In the current study, a method has been proposed for detection of DME.. As the cell has received enough of activating and inhibiting signal by synapses or dendrites .The cell accumulate these signal until a certain value called threshold value. The signal travel from cell to another by means of axons.. ANN classification of DME gives highest accuracy 96.43%, sensitivity 100% and specificity 92.86%.

### **Conclusion:**

High resolution SD-OCT radial scan is statically comparable to 3D-OCT scan in detection of DME. 3D-OCT is superior to radial OCT scan because the radial scan may lose a region of interest. Both scan has a varied correlation over the nine region .A novel macular edema detection algorithm shows highest accuracy 96.43%, sensitivity 100% and specificity 92.86%.

## **REFERNCES**

- [1] Mathew, C., Yunirakasiwi, A., & Sanjay, S. (2015). Updates in the management of diabetic macular edema. *Journal of diabetes research*, 2015.
- [2]Bhagat, N., Grigorian, R. A., Tutela, A., & Zarbin, M. A. (2009). Diabetic macular edema: pathogenesis and treatment. *Survey of Ophthalmology*; 54(1): 1-32.
- [3]-Mookiah, M. R. K., Acharya, U. R., Fujita, H., Tan, J. H., Chua, C. K., Bhandary, S. V., &Tong, L. (2015). Application of different imaging modalities for diagnosis of Diabetic Macular Edema: A review. *Computers in Biology and Medicine*; 66: 295-315.
- [4]Early Treatment Diabetic Retinopathy Study Research Group. (1987). Treatment techniques and clinical guidelines for photocoagulation of diabetic macular edema: EarlyTreatment Diabetic Retinopathy Study report number 2. *Ophthalmology*;94(7): 761-774
- [5] Huang, D., Swanson, E.A., Lin, C.P., Schuman, J.S., Stinson, W.G., Chang, W., Hee, M.R., Flotte, T., Gregory, K. and Puliafito, C.A.( 1991). Optical coherence tomography. *Science*; 254(5035):1178-1181.
- [6] Joel S. Schuman.(2012) "Introduction to Optical Coherence Tomography".
- [7] Massin P, Girach A, Erginay A, Gaudric A (2006) Optical coherence tomography: a key to the future management of patients with diabetic macular oedema. *Acta Ophthalmol Scand*; 84: 466-474
- [8] Tomlins, Peter H., and R. K. Wang. (2005)"Theory, developments and applications of optical coherence tomography." *Journal of Physics D: Applied Physics*; 38.15: 2519.
- [9] P. Serranho, M. Morgado, and R. Bernardes, (2012) "Optical Coherence Tomography: A Concept Review," in *Optical Coherence Tomography*, R. Bernardes and J. Cunha-Vaz, Eds. Springer-Verlag Berlin Heidelberg; 139–156.
- [10]Fercher, A. F., Drexler, W., Hitzenberger, C. K., & Lasser, T. (2003). Optical coherence tomography-principles and applications. *Reports on progress in physics*; 66(2): 239.
- [11]Eric H. Broecker, Mark T. Dunbar, (2005) "Optical Coherence Tomography: its clinical use for the diagnosis, pathogenesis, and management of macular conditions". *Optometry*, Elsevier ;76(2):79-101.

- [12] Nalina, P., & Muthukannan, K. (2013). Survey on image segmentation using graph based methods. *International Journal of Soft Computing and Engineering (IJSCE)*; 2231-2307.
- [13] Stephnie J. Chiu, Xiao T. Li, Peter Nicholas, Cynthia A. Toth, Joseph A. Izatt, SinaFarsiu(2010). "Automatic Segmentation of Seven Retinal Layers in SDOCT Images Congruent with Expert Manual Segmentation", *Optics Express*; 18(18):1943-19428.
- [14] J. Shi, and J. Malik, (2000) "Normalized Cuts and Image Segmentation," *IEEE Trans. Pattern Anal. Mach. Intell.* ; 22(8): 888–905.
- [15] K. Lee, M. Niemeijer, M. K. Garvin, Y. H. Kwon, M. Sonka, and M. D. Abramoff, (2010) "Segmentation of the optic disc in 3-D OCT scans of the optic nerve head," *IEEE Trans. Med. Imaging* ;29(1): 159–168 .
- [16] Haralick, R. M., Shanmugam, K. & Dinstein, I. (1973) Textural Features for Image Classification. *IEEE Transactions on Systems, Man, and Cybernetics* ;3: 610-621.
- [17] Rafeal C. Gonzalez, Richard E. Woods. (2009) "Digital Image Processing", 3rd Edition, Chapter 9, 10 & 11, pp. 627-833., ISBN: 978-81-317-2695-2, Prentice Hall.
- [18] S. Rajasekaran, G.A. Vijayalakshmi Pai, "Neural Network, Fuzzy Logic and Genetic Algorithm", Prentice Hall of India; 13-20.
- [19] Harsh Kukreja, Bharath N, Siddesh C S, & Kuldeep S. (2016). An Introduction to Artificial Neural Network. *International Journal of Advance Research and Innovative Ideas in Education* ; 1(5):27-30.
- [20] Hee, M. R., Puliafito, C. A., Wong, C., Duker, J. S., Reichel, E., Rutledge, B., ... & Fujimoto, J. G. (1995). Quantitative assessment of macular edema with optical coherence tomography. *Archives of ophthalmology*; 113(8):1019-1029.
- [21] Puliafito, C. A., Hee, M. R., Schuman, J. S., & Fujimoto, J. G. (2004). Optical coherence tomography of ocular diseases SLACK incorporated, 6900 grove road, Thorofare ; 3-34.
- [22] Lobo, C., Pires, I., & Cunha-Vaz, J. (2012). Diabetic macular edema. In *Optical Coherence Tomography* (pp. 1-21). Springer, Berlin, Heidelberg. [23] Sayanagi, Kaori et al. (2009) Comparison of Retinal Thickness Measurements Between Three-dimensional and Radial Scans on Spectral-Domain Optical Coherence Tomography *American Journal of Ophthalmology*; 148 : 431 - 438
- [24] Forooghian, F., Cukras, C., Meyerle, C. B., Chew, E. Y., & Wong, W. T. (2008). Evaluation of time domain and spectral domain optical coherence tomography in the measurement of diabetic macular edema. *Investigative ophthalmology & visual science*; 49(10): 4290-4296.
- [25] Polito A, Del Borrello M, Isola M, Zemella N, Bandello F. (2005) Repeatability and Reproducibility of Fast Macular Thickness Mapping With Stratus Optical Coherence Tomography. *Arch Ophthalmol.* ; 123(10):1330–1337.
- [26] Browning DJ, Glassman AR, Aiello LP, Beck RW, Brown DM, et al. (2007) Relationship between optical coherence tomography-measured central retinal thickness and visual acuity in diabetic macular edema. *Diabetic Retinopathy Clinical Research Network Ophthalmology*; 36: 114:525
- [27] Pham, D. L., Xu, C., & Prince, J. L. (2000). Current methods in medical image segmentation. *Annual review of biomedical engineering*; 2(1): 315-337.
- [28] Bezdek, J. C., Hall, L. O., & Clarke, L. (1993). Review of MR image segmentation techniques using pattern recognition. *Medical physics* ;20(4): 1033-1048.
- [29] Dutt, Vinita, Vikas Chaudhry, and Imran Khan. (2012) "Pattern recognition: An overview." *American Journal of Intelligent Systems*; 2.1: 23-27.
- [30] Zurada, J.M., 1992. Introduction to artificial neural systems St. Paul: West publishing company; 8.



- [31] Sengar, N., Dutta, M. K., Burget, R., & Povoda, L. (2015). Detection of diabetic macular edema in retinal images using a region based method. In 2015 38th International Conference on Telecommunications and Signal Processing (TSP); 412-415.
- [32] Kunwar, A., Magotra, S., & Sarathi, M. P. (2015, August). Detection of high-risk macular edema using texture features and classification using SVM classifier. In 2015 International Conference on Advances in Computing, Communications and Informatics (ICACCI) ;2285-2289.
- [33] Srinivasan, P. P., Kim, L. A., Mettu, P. S., Cousins, S. W., Comer, G. M., Izatt, J. A., & Farsiu, S. (2014). Fully automated detection of diabetic macular edema and dry age-related macular degeneration from optical coherence tomography images. *Biomedical optics express*; 5(10): 3568-3577.
- [34] Aftab, U., & Akram, M. U. (2012). Automated identification of exudates for detection of macular edema. In 2012 Cairo International Biomedical Engineering Conference (CIBEC) ;27-30.
- [35] Akram, M. U., Tariq, A., Khan, S. A., & Javed, M. Y. (2014). Automated detection of exudates and macula for grading of diabetic macular edema. *Computer methods and programs in biomedicine*; 114(2): 141-152.
- [36] Yang, Q., Reisman, C. A., Wang, Z., Fukuma, Y., Hangai, M., Yoshimura, N., ... & Chan, K. (2010). Automated layer segmentation of macular OCT images using dual-scale gradient information. *Optics express*; 18(20):21293-21307.
- [37] Hassan, B., & Raja, G. (2016). Fully automated assessment of macular edema using optical coherence tomography (OCT) images. In 2016 International Conference on Intelligent Systems Engineering (ICISE) ; 5-9.
- [38] Sheela, Basavaraj, L., & Akram, M.U. (2017). Diabetic Macular Edema Detection using Graph Theory and Retinal Layer Features. *International Journal of Engineering Trends and Technology*;49:363-368.

IJSER